

# Moving up in Frequency – D-Band the next frontier for Telecommunications XHaul

Dr Tudor Williams – Director of Technology  
Filtronic

## Abstract

*This paper explores why D-Band (130-175GHz) is required to enable next generation, ultra-high-capacity wireless links for 6G and beyond. Moving to D-Band is a fundamental shift and will require radical redesign due to the very high frequency of transmission. This paper will outline the challenges associated with manufacturing devices in volume at D-Band, with particular regard to MMIC-to-MMIC interconnects and MMIC-to-waveguide (WG) interfaces. Designs were completed for two types of MMIC-to-MMIC interconnects and two types of MMIC-to-WG interface with measured results showing promising performance for MMIC -to-WG with between 0.38 to 0.63 dB and 0.32 to 0.62 dB insertion loss respectively. Insertion loss of hot-via based MMIC-to-MMIC interconnection is found to be between 0.54 to 1.88 dB. Another MMIC-to-MMIC interconnection method using a piece of CPW quartz board achieves 0.31 to 1.08 dB insertion loss.*

## 1. Introduction

5G has already seen a shift in the frequency of mobile backhaul with significant take up of E-band to support dramatically increased subscribers and data rates. This is a trend that is set to continue. Figure 1 taken from a recent Ericson mobility report [1] shows the trend for fixed wireless access for fixed wireless access and mobile communications extending to 2027.

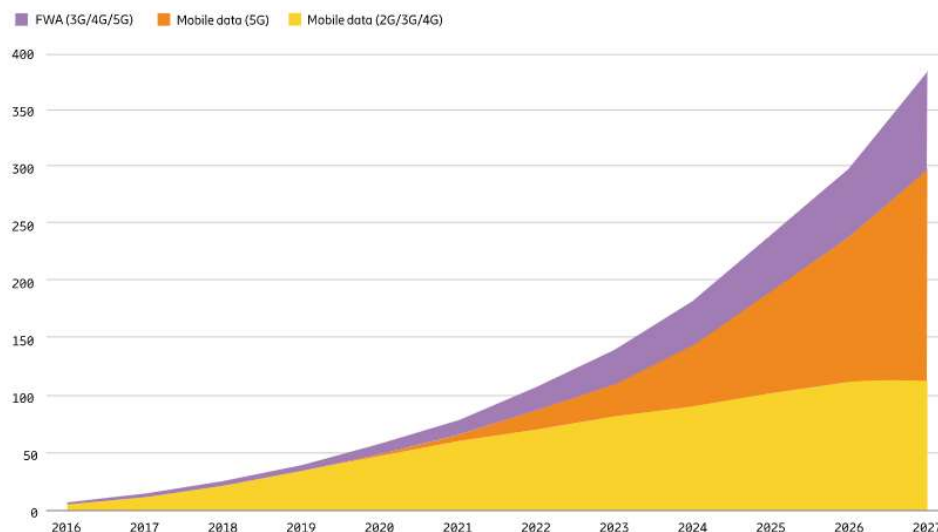


Figure 1.1 – Global Mobile Network Data traffic in EB per month (From Ericson Mobility Report 2021)

The next available band with sufficient spectrum would be W-band covering a frequency range from 92-114.5GHz, unfortunately due to other users of the spectrum this band will be split into smaller chunks and will mean that W-band will support only the same data rate as E-band. While this will be useful as E-band becomes congested, 6G and beyond will need massive capacity expanding to support increasingly diverse applications and services. New and wider bandwidths at frequencies in D-band (110-170 GHz) have been suggested as a potential solution to meet the higher data rate demand in the market [2][3]. There are however, many design challenges that need to be addressed to allow future D-band radio systems to be manufactured both economically and in volume. Chip-and-wire solutions are no longer appropriate at D-band as shown in the measurement result in Fig. 1. While a typical ground-signal-ground (GSG) ribbon bond connection between two MMICs could reduce the RF signal by less than 0 dB below 90 GHz, it incurs 3.1 dB insertion loss at 175 GHz.

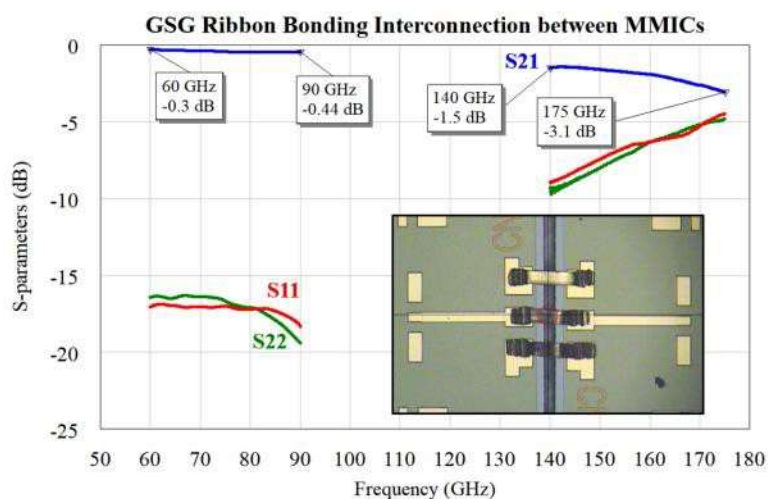


Figure 1.2 – Measured S-parameters of a 100µm pitch ground-signal-ground (GSG) ribbon bonding connection between two MMICs at 60-90 GHz and 140- 175 GHz.

Reactive matching on the MMICs could in principle mitigate the mismatch loss, however this is not practical in a volume production environment. The variability in tape length, MMIC placement, loop height etc. is too wide to guarantee a high production yield at 175GHz with fixed matching structures.

There are significant challenges around interconnects for both MMIC-to-MMIC connections and MMIC-to-WG. This paper will propose and demonstrate alternative low loss, highly repeatable direct MMIC-to-WG and MMIC-to-MMIC interconnections thereby eliminating highly variable bond wires/tapes. Two types of direct MMIC-to-WG transitions and two types of MMIC-to-MMIC interconnections have been designed, fabricated, assembled, and tested. A built-in hot-via technology in the MMIC process and a piece of CPW quartz board are used for the two types of the MMIC-to-MMIC interconnections. As practical mmWave assemblies require transitions to WG elements in either parallel or perpendicular directions relative to the MMIC surface two MMIC-to-WG transition have been designed and realised to address these requirements and realised with the help of a periodic EBG structure on the test fixture covers.

## 2. Design of 140-175GHz MMIC-to-WG transitions

### 2.1 Cavity Modes - Electromagnetic bandgap (EBG) Structure Design

As we move to very short wavelengths cavity resonances can become a significant issue. One solution is Electromagnetic Band-Gap (EBG) materials which have been studied for many years. It has been used in antenna designs, high-isolation electronic packages, stealth technology, and gap waveguide [4]. An artificial magnetic conductor (AMC) layer realised with a periodic metal pin array structure can effectively suppress all unwanted parallel-plate modes inside a cavity [6]. We have modelled and measured such pin arrays and used these within the designs described below.

### 2.2 MMIC-to-Waveguide Transition design – Type 1

Fig. 2.1 and 2.2 show the back-to-back 3D EM model and split block test fixture of Type-1 MMIC-to-WG transition. Two WR5 (140-220 GHz) waveguide connections are at the bottom of the MMIC carrier (Fig. 2.1c). A MMIC (Fig. 2.1b) with two waveguide transition probes and a 2.2 mm long 50  $\Omega$  microstrip line sits on the carrier. The wave propagates through the waveguide perpendicular to the MMIC surface and is coupled to the transition probe. There are vias in the MMIC around the transition area to minimise the signal leakage. The MMIC backside layer is patterned so no metal except the transition probe is overhung above the waveguide. The cover (Fig. 2.1a) contains back-shorts of the waveguide and the AMC pin array. All the WR5 waveguide features have been designed with corners of a 0.25 mm radius to aid volume manufacture of the metalwork.

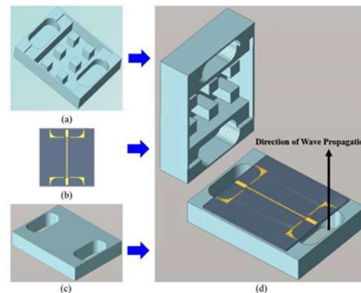


Fig. 2.1. Type-1 MMIC-to-WG transition back-to-back 3D EM model: (a) cover with WG backshorts and AMC pin array; (b) MMIC with two transition probes and a microstrip line; (c) MMIC carrier with WR5 WG connections; (d) 3D view of the model.

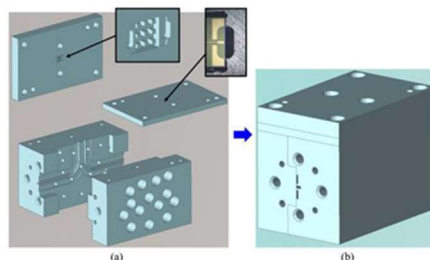
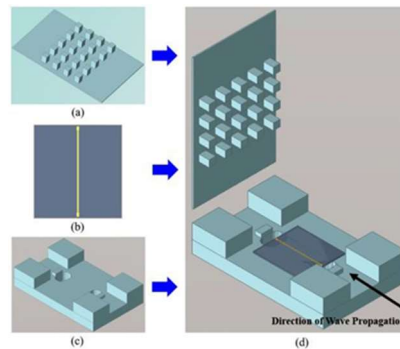


Fig. 2.2. Type-1 MMIC-to-WG transition test fixture: (a) metalwork pieces of the test fixture; (b) 3D model of the whole assembly.

### 2.3 MMIC-to-Waveguide Transition design – Type 2

Back-to-back 3D EM model and split block test fixture of Type-2 MMIC-to-WG transition is shown in Fig. 2.3 and 2.4 respectively. The same concept of the transition has been demonstrated at 80 to 114 GHz [6]. There are two resonant cavities, two capacitive posts, and two WR5 waveguide connections in the MMIC carrier (Fig. 2.3c). The MMIC (Fig. 2.3b) contains two waveguide transition probes and a 1.6 mm long 50  $\Omega$  microstrip line. The wave propagates through the waveguide parallel to the MMIC surface and is coupled to the transition probe thanks to the resonant cavity and the capacitive post in the carrier, and the AMC pin array in the cover (Fig. 2.3a). MMIC backside layer is patterned so no metal except the transition probe is overhung above the cavity. The cover also acts as the top metal wall of the WR5 waveguide.



**Fig. 2.3 - Type-2 MMIC-to-WG transition back-to-back 3D EM model: (a) cover with AMC pin array; (b) MMIC with two transition probes and a microstrip line; (c) MMIC carrier with two capacitive posts, two coupling cavities, and two WR5 WG connections; (d) 3D view of the model.**

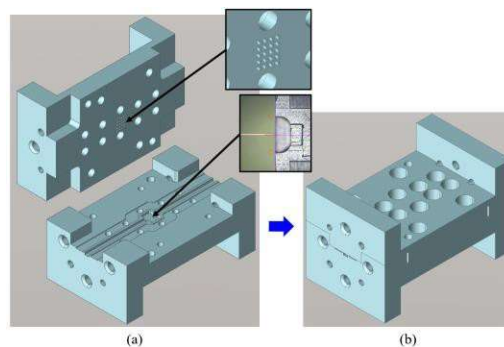


**Fig. 2.4. Type-2 MMIC-to-WG transition test fixture: (a) metalwork pieces of the test fixture; (b) 3D model of the whole assembly.**

### 3. Design of 140-175GHz MMIC-to-MMIC Interconnections

#### 3.1 MMIC-to-MMIC Transition design – Type 1

A process with built-in RF hot-via technology from WIN Semiconductor has been chosen for the Type-1 MMIC-to-MMIC interconnection design. While standard through-wafer vias provide ground connections, hot-vias enable the connection between the RF track on the topside of the MMIC and the RF port on the backside of the MMIC. MMIC backside metal needs to be patterned to separate the RF port and the ground.

Fig. 3.1 and 3.2 show the 3D EM model and test fixture of the Type-1 MMIC-to-MMIC interconnection with hot-vias. 50  $\Omega$  microstrip lines on the topside of the MMICs are connected to the backside CPW ports by 4 hot-vias as shown in Fig. 3.1a and Fig. 3.1d. The two MMIC backside CPW ports are then connected by the CPW tracks on a PCB carrier (Fig. 3.1b). A clear view of the RF tracks and hot-vias is shown in Fig. 3.1d.

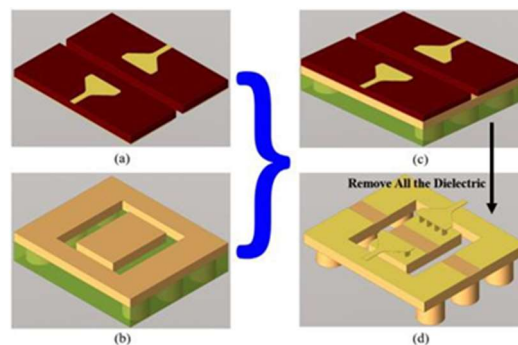


Fig. 3.1. Type-1 MMIC-to-MMIC interconnection with hot-vias: (a) two MMICs with hot-via interconnection structure; (b) PCB carrier for the MMICs; (c) 3D EM model; (d) MMIC and PCB dielectric removed for clear view of the interconnection.

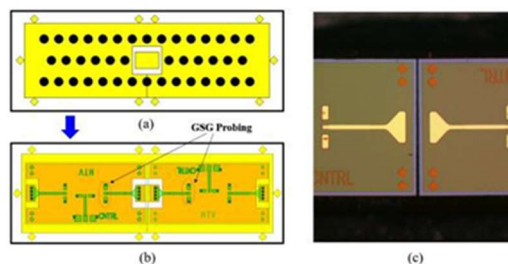
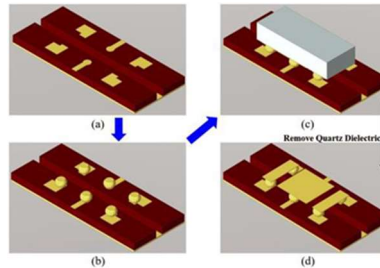


Fig. 3.2. Type-1 MMIC-to-MMIC interconnection test fixture [6]: (a) PCB carrier with CPW tracks; (b) assembly diagram of two MMICs on the PCB carrier; (c) top view of the test fixture.

#### 3.2 MMIC-to-MMIC Transition design – Type 2

A quartz substrate with CPW tracks is used to provide the interconnection between MMICs in the Type-2 design. 3D EM model and a picture of the test fixture are shown in Fig. 3.3 and 3.4 respectively. Quartz is chosen as the substrate material because of its low dielectric constant and transparency for easy alignment. To achieve the proposed assembly, metal bumps are placed on

the MMIC GSG pads (Fig. 3.3b). Then the quartz substrate can be attached to the bumps by thermocompression bonding with carefully controlled process temperature (Fig. 3.3c). Compared to the impedance mismatch caused by the inductance and parasitics of the traditional bonding wires, the mismatch in this method can be minimised by accurate design and tuning of the CPW structure on the quartz substrate.



**Fig. 3.3.** Type-2 MMIC-to-MMIC interconnection with CPW quartz board: (a) two MMICs with GSG bonding pads; (b) Metal bumps are placed on the MMIC pads; (c) 3D view of the model; (d) Quartz dielectric removed for clear view of the interconnection.

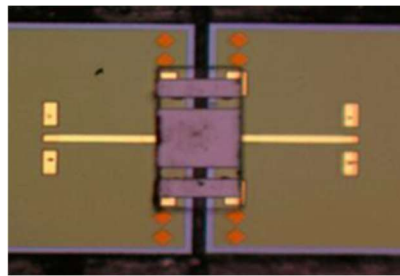


**Fig. 3.4.** Top view of Type-2 MMIC-to-MMIC interconnection test fixture [6].

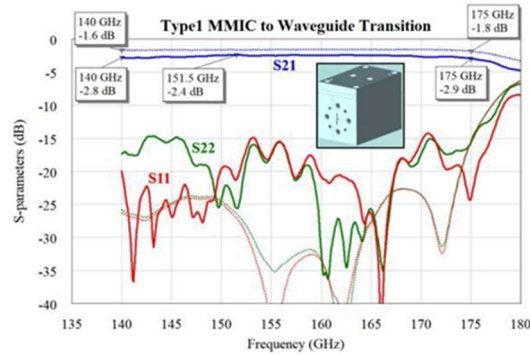
## 4. Experimental Results

The measurements were carried out using a Keysight PNA-X with two VDI WR5 frequency extension modules. Waveguide TRL (Thru-Reflect-Line) calibrations were performed prior to the measurements of MMIC-to-WG transitions. For measurement of MMIC-to-MMIC interconnections, the above VNA was used together with a pair of WR5 to D-band tapered waveguides, and a pair of D-band GGB Picoprobe. On-wafer TRL calibration was undertaken using the standards fabricated on the same wafer as the MMICs. TRL was chosen due to its minimal requirement on prior knowledge of the custom standards on the wafer and its ability to move reference planes to the devices under test.

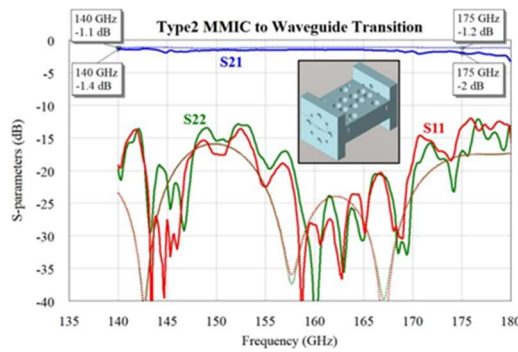
WR5 waveguide thrus for the two MMIC-to-WG transition test fixtures have been fabricated and measured. Type-1 and Type-2 thrus generated about 1 dB and 0.3 dB insertion loss respectively between 140 to 175 GHz. Measurement of a 1.4 mm long 50  $\Omega$  microstrip line on the MMIC showed about 0.4 dB insertion loss in the same frequency range. Individual MMIC-to-WG transition loss can therefore be obtained by de-embedding the back-to-back test fixture.

Fig. 4.1 and 4.2 show the simulations and measured S- parameters of the Type-1 and Type-2 MMIC-to-WG back-to-back transition test fixtures respectively. 2.4 to 2.9 dB insertion loss was measured for type-1 transition between 140 to 175 GHz. After de-embedding the WR5 waveguide

in the test fixture and a 2.2 mm long 50  $\Omega$  microstrip line on the MMIC, it is estimated the loss per transition is between 0.38 to 0.63 dB. In the same frequency range type-2 transition test fixture exhibits 1.4 to 2 dB insertion loss in the measurement. The individual transition loss is considered to be between 0.32 to 0.62 dB after de-embedding WR5 waveguide and a 1.6 mm long 50  $\Omega$  microstrip line.



**Fig. 4.1.** Simulation and measured S-parameter results for the back-to-back test fixture of Type-1 MMIC-to-WG transition. Dotted curves: simulation result; solid curves: measurement result.



**Fig. 4.2.** Simulation and measured S-parameter results for the back-to-back test fixture of Type-2 MMIC-to-WG transition. Dotted curves: simulation result; solid curves: measurement result.

Fig. 4.4 shows the measurement result of 0.66 to 2 dB insertion loss for the Type-1 MMIC-to-MMIC interconnection test fixture with hot-vias. The loss caused by the interconnection itself is then considered to be between 0.54 to 1.88 dB after de-embedding two 0.2 mm long 50  $\Omega$  microstrip lines on the MMIC. Type-2 MMIC-to-MMIC interconnection test fixture based on CPW quartz board exhibits better insertion loss of 0.43 to 1.2 dB as shown in Fig. 4.4. After de-embedding the 50  $\Omega$  microstrip lines on the MMIC, 0.31 to 1.08 dB loss is achieved for the interconnection itself.



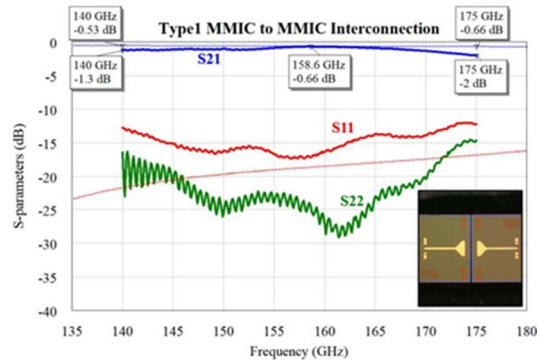


Fig. 4.3. Simulation and measured S-parameter results for the test fixture of type-1 MMIC-to-MMIC interconnection. Dotted curves: simulation result; solid curves: measurement result.

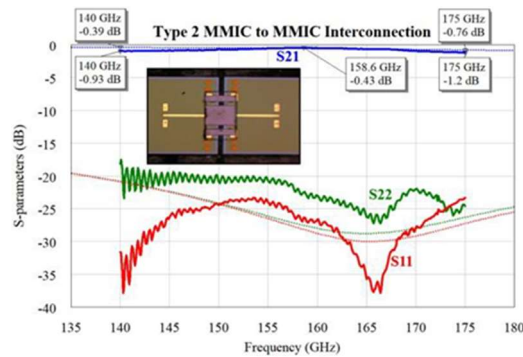


Fig. 4.4. Simulation and measured S-parameter results for the test fixture of type-2 MMIC-to-MMIC interconnection. Dotted curves: simulation result; solid curves: measurement result.

## 5. Conclusion

This paper has reviewed the integration constraints of future D-band radio systems. We then demonstrated two types of direct MMIC-to-WG transitions with EBG structures integrated in the cover, and two types of bonding wire free MMIC-to-MMIC interconnections using hot-vias and CPW quartz board. Low insertion loss and good return loss has been achieved for all the proposed solutions between 140 and 175 GHz

## References

- [1] Ericson Mobility Report, November 2021. <https://www.ericsson.com/en/reports-and-papers/mobility-report/reports/november-2021>
- [2] Ericsson Microwave Outlook Report (2017). [Online]. Available: <https://www.ericsson.com/en/reports-and-papers/microwave-outlook>
- [3] M. Frecassetti, P. Roux, A. Lamminen, J. Saily, J. Sevillano, D. del Rio, and V. Ermolov, "D-band radio solutions for beyond 5G reconfigurable meshed cellular networks," in Proc. International Symposium on Wireless Communication Systems, 2019, pp. 427-431.



- [4] P. Kilda, "Gap waveguides and PMC packaging: octave bandwidth mm- and submm-Wave applications of soft & hard surfaces, EBGs and AMCs," in Proc. Forum for Electromagnetic Research Methods and Application Technologies, 2015, vol. 11.
- [5] A. Zaman, M. Alexanderson, T. Vukusic, and P. Kildal, "Gap waveguide PMC packaging for improved isolation of circuit components in high-frequency microwave modules," IEEE Transactions on Components, Packaging and Manufacturing Technology, vol. 4, no. 1, pp. 16-25, Jan. 2014.
- [6] A. Zaman, V. Vassilev, H. Zirath, and N. Rorsman, "Novel low-loss millimeter-wave transition from waveguide-to-microstrip line suitable for MMIC integration and packaging," IEEE Microwave and Wireless Components Letters, vol. 27, no. 12, pp. 1098-1100, Dec. 2017.
- [7] C. Buck, J. Ding, N. Ridler, and X. Shang, "Ultra high frequency interconnects for compound semiconductors," Final report for Innovate UK project 103438, Jan. 2019.